Machine-Learning Discovery of Highly Oxidized IrO_x Phases

Raul A. Flores,[*,†] Christopher Paolucci,[*,‡] Ankit Jain,[*,¶] Muratahan Aykol,[*,§] Jens K. Nørskov,[*,¶] Michal Bajdich,[*,‖] and Thomas Bligaard[*,‖]

† *SUNCAT Center for Interface Science and Catalysis, Department of Chemical Engineering, Stanford University, Stanford 94305, California, USA*
‡ *Department of Chemical Engineering, University of Virginia, Charlottesville, Virginia 22903, United States*
¶ *Department of Physics, Technical University of Denmark, Lyngby, Denmark*
§ *Toyota Research Institute, Los Altos, CA 94022, USA*
‖ *SUNCAT Center for Interface Science and Catalysis, SLAC National Accelerator Laboratory, Menlo Park, CA 94025, USA*

E-mail: flores12@stanford.edu; cp9wx@virginia.edu; temp_temp_ankits_email_address_temp_temp@dtu.dk; muratahan.aykol@tri.global; jkno@dtu.dk; bajdich@slac.stanford.edu; bligaard@stanford.edu

Results and discussion

III. Electrochemical OER Application

In the following section we will demonstrate the merit of our stable polymorph discovery algorithm by elucidating the electrochemical properties of the four promising structures discussed in the previous section. In particular, surfaces constructed from the four polymorphs will be evaluated for their activity towards the oxygen evolution reaction (OER), an important chemistry with direct application to fuel cell devices. Additionally, the surfaces will be evaluated for their stability and equilibrium surface coverage of surface oxygen and hydroxides.

Bulk Pourbaix

The electrochemical stability phase diagram (E vs. pH) was constructed by considering the equilibrium conditions of the following species: Ir, rutile-IrO_2 , α-IrO_3 , rutile-IrO_3 , β-IrO_3 , and an aqueous dissolved IrO[4−] species (See TEMP—SI for additional details). The resulting diagram is shown in Fig. S1. Importantly, under acidic conditions (pH <7) and in the bias region of interest for the OER (1.23 V vs. RHE) α-IrO_3 shows a large window of stability. This indicates that the α-IrO_3 phase may be stabilized under the highly oxidizing conditions of the OER. For comparison, the stability regions of the metastable rutile-IrO_3 and β-IrO_3 phases, in the absence of any other competing IrO_3 polymorphs, are indicated by unfilled solid lines. As shown, these metastable phases appear to also have a wide region of stability in the OER region, due to to their formation energies being within TEMP eV of the globally stable α-IrO_3 phase, see SI table TEMP for the bulk energies of all considered phases. Because of their similar energies it is possible that some or all of these IrO_3 phases may be present and relevent for the OER. In the next section, we explore this possibility by computing the theoretical OER activity of these polymorph systems.

[Figure 1 about here.]

b. OER Activities and Surfaces

Fig. S2 summarizes the major results of the electrochemical activity and surface stability analysis. First, Fig. S2 a.) shows the surace energy Pourbaix plots for the four IrOx crystals of interest. For each bulk system, the surface energy as a function of applied potential (pH=0), for various facets, and at various coverages (bare, *OH, and *O covered), are shown, see SI for more details. The specific facets were chosen from the highest intensity x-ray diffraction peaks from powder-diffraction spectra simulated in VESTA, as well as using physical intuition as to which facets would be most physical. Additionally, the bulk phase limits of stability from figure TEMP are included at the bottom of each subplot. In most cases, the oxygen covered surfaces dominate at the OER equilibrium potential (1.23 V vs RHE) with bare surfaces being competitive to within TEMP eV/A2, this competitivness goes away at even modest overpotentials (eta 0.3, –¿ 1.5 V vs RHE), at which point the oxygen covered terminations are further overstabalized relative to the bare surfaces, making them the sole dominant termination. Therefore in our activity analysis we consider mainly oxygen terminated surfaces for the OER. The OER activity (expressed in terms of the limiting potential) for select oxygen terminated surfaces are shown in Fig. S2 as a function of the DGO-DGOH TEMP OER thermodynamic descriptr. The two rutile-IrO2 suraces (100, and 110) are located towards the strong binding side of the volcano, indicating that that they bind OER intemediate too strongly. Encourangly, with predicted overpotentials of TEMP and TEMP, our rutile-IrO2 are within the range of experimental overpotentials found in literature. The three IrO3 polymorph surfaces all have DGO-DGOH descriptor towards the top and right of the volcano, indicative of weaker binding energetics. This is evident from figure SI TEMP (scaling) which shows a clear distinction between the IrO2 and IrO3 polymorphs, with IrO3 binding overall weaker than IrO2. The best performing systems, including the (100), (110), and (211) facets of a-IrO3, b-IrO3 (101), and R-IrO3 (110), have overpotentials of 0.4 V vs RHE, a 0.2 V vs RHE improvemnt over the rutile-IrO2 system.

[Figure 2 about here.]

c. OER Intermediate Scaling

Figure TEMP shows the scaling relations between the adsorption free energies of the OER intermediate species for the IrO_x systems studied herein. It can be seen clearly that the data points corresponding to the three IrO_3 polymorphs are roughly 1 eV weaker binding than the rutile-IrO_2 points. This generally weaker binding of the IrO_3 stoichiometry is responsible for the observed improvement in theoretical activity. The ΔG_{OOH} vs.ΔG_{OH} relationship is very close to the traditional "universal scaling relations", demonstrating that our materials do not break the infamous ΔG_{OOH} vs. ΔG_{OH} scaling.

[Figure 3 about here.]

Conclusion

And in conclusion we presented work here...

Acknowledgement Organizations to acknowledge TRI SUNCAT Stanford NERSC etc. JAGT and MB acknowledge the support by the U.S. Department of Energy, Office of Science, Office of Basic Energy Science, via Grant DE-SC0008685 to the SUNCAT Center of Interface Science and Catalysis. The authors would like to acknowledge the use of the computer time allocation for the Transition metal-oxide and metal surfaces: applications and reactivity trends in catalysis at the National Energy Research Scientific Computing Center, a DOE Office of Science User Facility supported by the Office of Science of the U.S. Department of Energy under Contract No. DE-AC02-05CH11231.

References

.

List of Figures

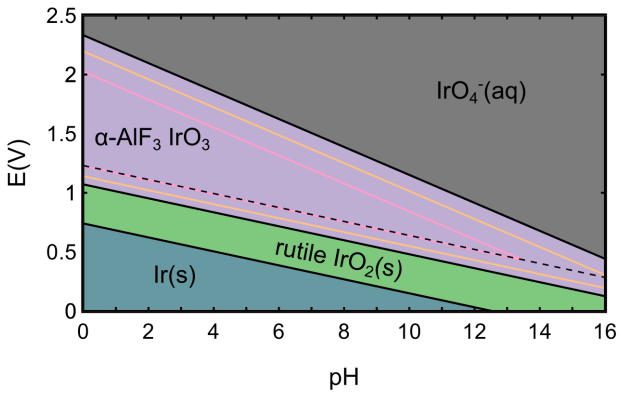

Figure S1: , Electrochemical bulk phasetability diagram (Pourbaix) of the Ir-O-H chemical space with respects to changes in potential and pH. We considered a bulk unoxidized Ir(s) (blue), a [+4] rutile-IrO_2 (green), and an aqueously dissolved IrO[4−] (grey) phase. Additionnally, we considered the three IrO_3 polymorphs, α-IrO_3 (purple), rutile-IrO_3 (orange), and β-IrO_3 (pink). The water equilibrium line at 1.23 V vs RHE, which corresponds to a 0 overpotential catalyst, is shown by a dotted line.

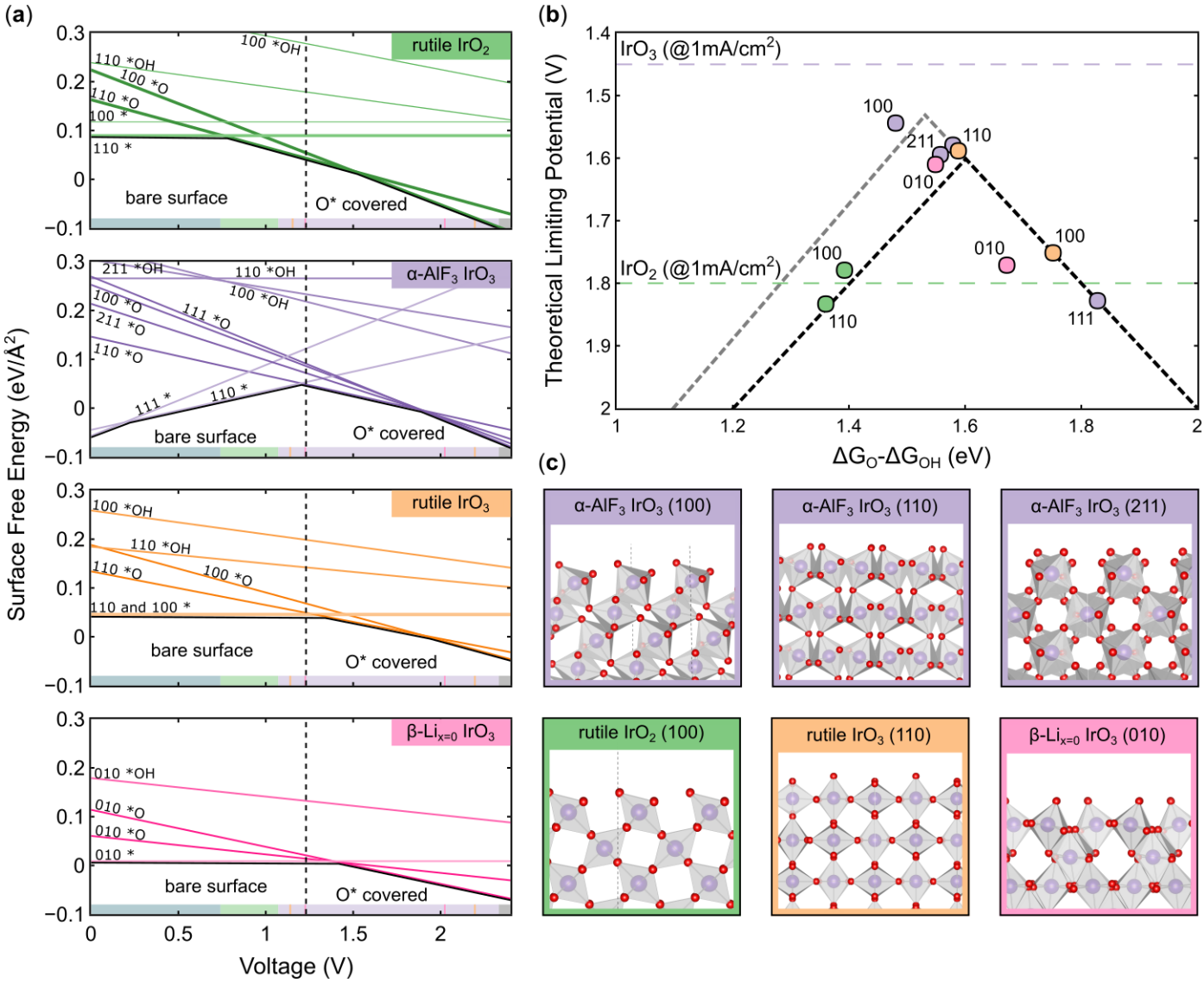

Figure S2: Summary of OER results for the four bulk structures of IrO_x considered: rutile-IrO_2 (green), α-IrO_3 (purple), rutile-IrO_3 (orange), and β-IrO_3 (pink). (a) Surface energy Pourbaix diagrams for each structure, with the surface energy of various facets and coverages shown as a function of applied potential. The bulk Pourbaix diagram's bounds of stability at pH 0 are superimposed at the bottom of each subplot. (b) OER activity volcano for IrO_x systems considered utilizing the ΔG_O -ΔG_{OH} thermodynamic descriptor. The purple dotted line corresponds to the experimental limiting potential at 10 mA cm^2 for IrO_3, while the green band corresponds to the range of experimentally observed overpotentials for pristine IrO_2 catalysts. (c) Select surface facets for the four IrO_x crystal systems considered.

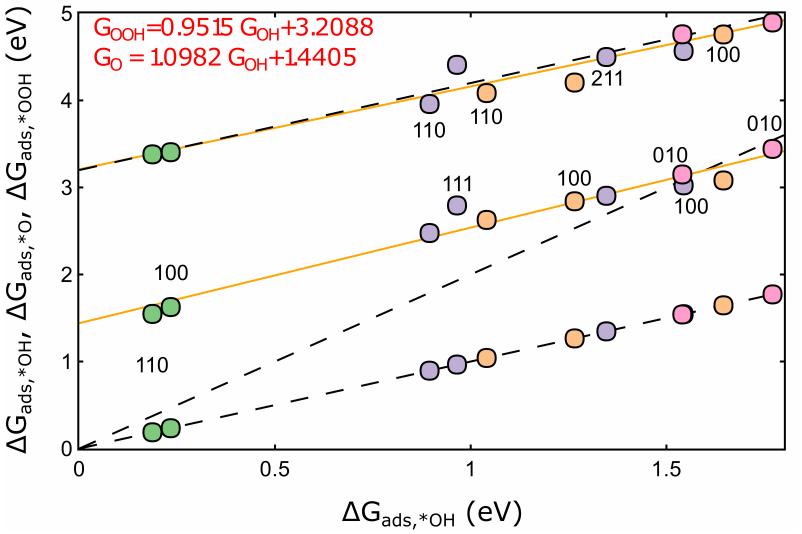

Figure S3: Relationship between the adsorption free energies of the three key OER intermediates (*OH, *O, *OOH), with ΔG_{OH} chosen as the dependent variable. Best fit lines are provided for ΔG_{OOH} vs. ΔG_{OH} and ΔG_{O} vs. ΔG_{OH} . Additionally, "universal scaling relations" for ΔG_{OOH} vs. ΔG_{OH} and ΔG_{O} vs. ΔG_{OH} are shown (black dotted lines) to emphasize our deviation from the traditionally reported scaling fits. The trivial ΔG_{OH} vs. ΔG_{OH} relationship is included for completeness.

Graphical TOC Entry